Molecular Therapy
Nucleic Acids
Original Article

Highly efficient nucleic acid encapsulation method for targeted gene therapy using antibody conjugation system

Seokbong Hong,[1,3] Seung-hwan Jeong,[1,2,3] Jang Hee Han,[1,2] Hyeong Dong Yuk,[1,2] Chang Wook Jeong,[1,2] Ja Hyeon Ku,[1,2] and Cheol Kwak[1,2]

[1]Department of Urology, Seoul National University College of Medicine, 03080 Seoul, South Korea; [2]Department of Urology, Seoul National University Hospital, 03080 Seoul, South Korea

Gene therapy has surfaced as a promising avenue for treating cancers, offering the advantage of deliberate adjustment of targeted genes. Nonetheless, the swift degradation of nucleic acids in the bloodstream necessitates an effective and secure delivery system. The widespread utilization of poly(lactic-co-glycolic acid) (PLGA) nanoparticles as drug delivery systems has highlighted challenges in controlling particle size and release properties. Moreover, the encapsulation of nucleic acids exacerbates these difficulties due to the negatively charged surface of PLGA nanoparticles. In this study, we aimed to improve the encapsulation efficiency of nucleic acids by employing negatively charged microbeads and optimizing the timing of the specific formulation steps. Furthermore, by conjugating PSMA-617, a ligand for the prostate-specific membrane antigen (PSMA), with PLGA nanoparticles, we assessed the antitumor effects and the efficacy of a nucleic acid delivery system on a prostate cancer model. The employed technique within the nucleic acid encapsulation system represents a novel approach that could be adapted to encapsulate various kinds of nucleic acids. Moreover, it enables the attachment of targeting moieties to different cell membrane proteins, thereby unveiling new prospects for precise therapeutics in cancer therapy.

INTRODUCTION

PLGA (poly(lactic-co-glycolic acid)) is a highly biocompatible and biodegradable material. When introduced into the body, PLGA is broken down into lactic and glycolic acids, which are subsequently absorbed.[1] Hence, PLGA is widely utilized in the development of drug delivery systems, and its safety has been validated by its inclusion in commercially available drugs such as Zoladex (Goserelin) and Lupron Depot (Leuprorelin).[2] Although PLGA has been successfully employed for the encapsulation of small chemically active pharmaceutical ingredients (APIs), the encapsulation of nucleic acids is challenging. Nucleic acids possess a phosphate group in their backbone that results in a strong negative charge.[3] Similarly, PLGA generally has a negative surface charge, leading to electrical repulsion during the formulation process.[4] Consequently, encapsulating nucleic acids within PLGA is challenging because of these electrostatic interactions.

Various nucleic acids, such as DNA, mRNA, siRNA, and miRNA, can serve as APIs in gene therapy delivered by nanoparticles.[5] However, the efficient delivery of carriers is required to overcome the challenges associated with gene therapy. To address this limitation, we developed a method to achieve highly efficient encapsulation of nucleic acids within PLGA nanoparticles conjugated with prostate-specific membrane antigen (PSMA) ligands, thereby overcoming delivery hurdles.[4,6]

PSMA is a membrane protein predominantly expressed in normal prostate epithelial cells and PSMA expression increases significantly in prostate cancer cells, ranging from 100 to 1,000 times higher than that in normal prostate epithelial cells.[7,8] Leveraging these unique characteristics, PSMA-based theragnostic, diagnostic, and therapeutic approaches have been extensively explored.[2,9,10]

In this study, we employed the PSMA ligand, specifically PSMA-617, conjugated onto PLGA nanoparticles to precisely deliver siRNAs to prostate cancer cells.[11–13] We demonstrated the anticancer efficacy of gene therapy in a prostate cancer model, highlighting the success of our highly efficient nucleic acid encapsulation system.

RESULTS

Factors that increase the encapsulation rate in the formulation of PLGA nanoparticles containing nucleic acids

Encapsulating nucleic acids within PLGA poses a challenge because most APIs developed using PLGA as a drug delivery system are small chemicals. This difficulty arises from the strongly negative charge of nucleic acids, which is attributed to the presence of a phosphate group in their backbone. Similarly, PLGA formulations typically exhibit negatively charged surfaces, leading to electrostatic repulsion between PLGA and nucleic acids. Consequently, encapsulating nucleic acids

Received 4 February 2024; accepted 3 September 2024;
https://doi.org/10.1016/j.omtn.2024.102322.

[3]These authors contributed equally

Correspondence: Cheol Kwak, Department of Urology, Seoul National University Hospital, 03080 Seoul, South Korea.
E-mail: mdrafael@snu.ac.kr

Published by Elsevier Inc. on behalf of The American Society of Gene and Cell Therapy.
This is an open access article under the CC BY-NC-ND license (http://creativecommons.org/licenses/by-nc-nd/4.0/).

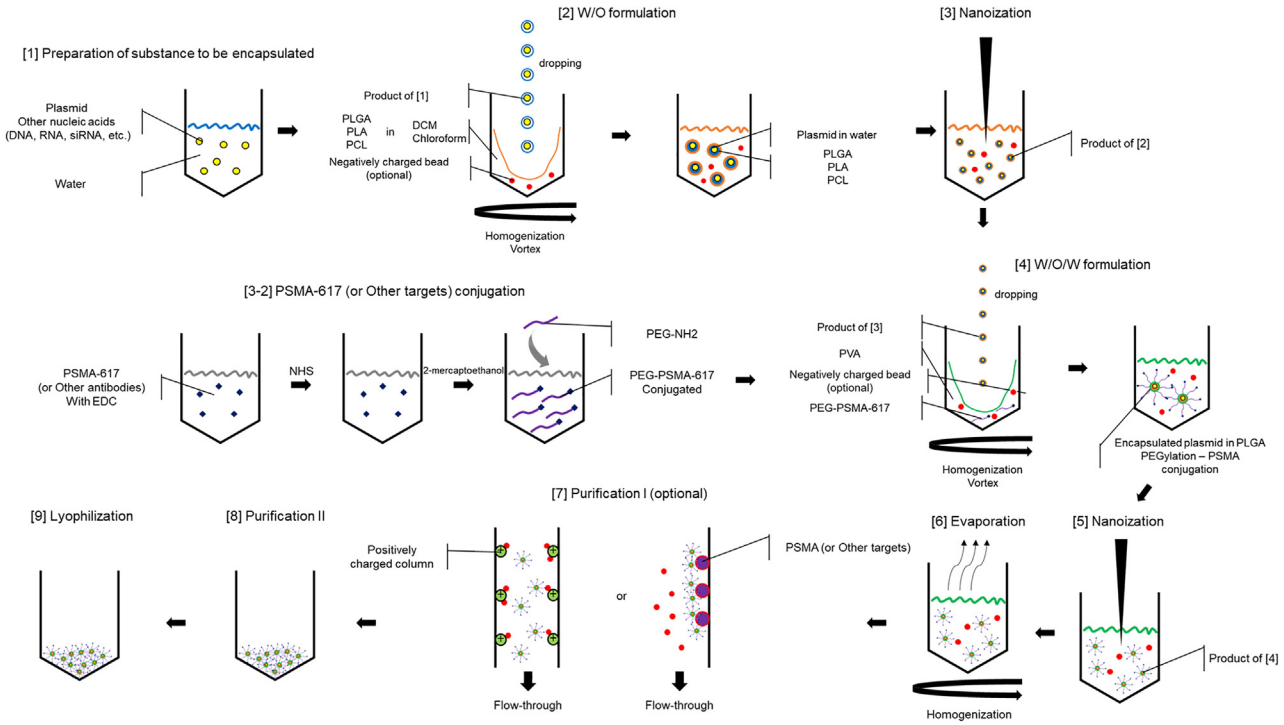

Figure 1. Schematic diagram of the entire process of PLGA nanoparticle formulation for high-efficiency nucleic acid encapsulation

The method of formulating PLGA nanoparticles to encapsulate nucleic acids such as plasmids and siRNA, and the technique for conjugating substances capable of targeting specific biomolecules. This formulation encapsulates plasmids to achieve a diameter of approximately 500 μM, and the nanoparticle surface is based on a formulation method that conjugates PSMA-617. The encapsulation method for other nucleic acids such as siRNA follows the same procedure, with the diameter determined by the concentration levels of PLGA, PVA, etc. This is detailed in Figure S2. The conjugation is recorded based on PSMA-617, and the attachment of other materials such as antibodies may require precise methodological adjustments depending on the case. PLGA, poly(lactic-co-glycolic acid); PLA, polylactic acid; PCL, polycaprolactone; PEG, polyethylene glycol; DCM, dichloromethane; EDC, 1-ethyl-3-[3-dimethylaminopropyl]carbodiimide hydrochloride; NHS, N-hydroxysuccinimide.

within PLGA nanoparticles is highly challenging because of electrical repulsion.

One key formulation method employed to enhance the encapsulation rate of nucleic acids involves the use of cations, such as calcium,[14] which has demonstrated a high success rate of approximately 33%–50% compared with the initial input. In this study, we propose an alternative method that achieves highly efficient encapsulation of nucleic acids, which is distinct from conventional cation-based formulation approaches. Furthermore, we incorporated substance-PEG conjugation during nanoparticle preparation to enable the specific targeting of cell membrane proteins. This approach aims to address the limitations of conventional PLGA nanoparticles, which rely heavily on the enhanced permeability and retention (EPR) effect when used as delivery vehicles for anticancer drugs, but face challenges when applied to scenarios with limited EPR effects, such as prostate cancer.[15]

The water-in-oil-in-water (W/O/W) formulation method was used for the encapsulation of hydrophilic substances, such as nucleic acids, and nanoization was performed using sonication. Owing to the nature of PLGA, the release time of internal substances in the blood can be controlled by adjusting the ratio of lactic acid to glycolic acid, the use of polycaprolactone (PCL), and its molecular weight.[16] The important factors for the high encapsulation rate of nucleic acids that can be derived from the results of this study are (1) the concentration of PLGA dissolved in the DCM solvent, (2) the concentration of PVA, (3) the transition time from the formulation step [2, 4] to the nanoization step [3, 5], and (4) the use of negatively charged microbeads. The key factors that greatly affect the nucleic acid encapsulation rate are the transition time from the formulation step [2, 4] to the nanoization step [3, 5] and the use of negatively charged microbeads (Figure 1). The plasmid encapsulation rate of the PLGA nanoparticles was improved from 9% to 61% by adjusting these two factors (Figures 2B and 2C).

To measure the efficiency of siRNA encapsulation in PLGA nanoparticles, the nanoparticles were formulated with siRNA using the method described in Figure 1, followed by quantification to assess the encapsulation rate. After formulation, the PLGA was dissolved using DCM solvent to release the siRNA, and the quantification method employed was that of Chen et al.[17] The concentration of input siRNA used in the formulation was 1 nM, and the test was repeated three times, yielding concentration results of 0.6799, 0.8879, and

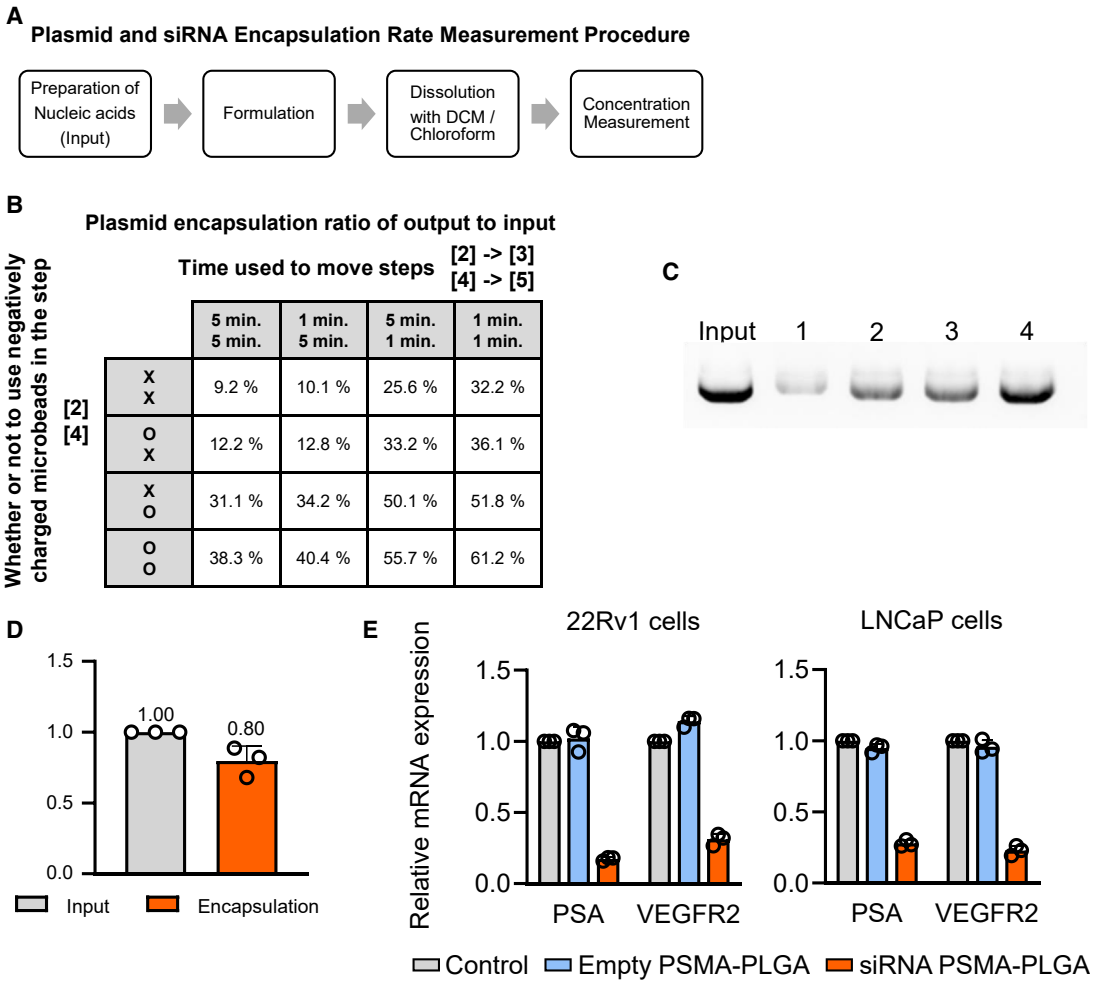

Figure 2. Plasmid and siRNA encapsulation rate of formulated PLGA nanoparticles

(A) Experimental procedure for measuring encapsulation rate. (B) Encapsulation rate table according to the time until the start of the nanoization step and the use of negatively charged beads, which are the two factors that have the greatest impact on the plasmid encapsulation rate. (C) PCR results enabling the visual confirmation of plasmid encapsulation rates under each condition. Representative conditions of the encapsulation rate measurement table. (1) Sufficient time (5 min) before nanoization and no negatively charged particles. (2) Fast time until nanoization (1 min) and no negatively charged particles. (3) Sufficient time (5 min) before nanoization and use of negatively charged particles. (4) Fast time until nanoization (1 min) and use of negatively charged particles. (D) Results for the encapsulation efficiency of siRNA when using PLGA nanoparticles. (E) siRNA delivery by PSMA-617-conjugated PLGA nanoparticles in the prostate cancer cell lines 22Rv1 and LNCaP cells. PLGA, poly(lactic-co-glycolic acid); DCM, dichloromethane.

0.8217 nM, with an average value of 0.7965 nM, indicating a high encapsulation rate (Figure 2D).

To verify the effectiveness of encapsulation and precise delivery of siRNA by PSMA-617-conjugated PLGA (PSMA-PLGA) nanoparticles, two prostate cancer cell lines were utilized. The prostate cancer cell lines, 22Rv1 and LNCaP, were treated for 48 h with PSMA-PLGA nanoparticles encapsulating either scrambled siRNA as a control or siRNAs designed to knock down *PSA* and VEGF receptor 2 (*VEGFR2*), respectively (Figure 2E). It was revealed that PSMA-PLGA nanoparticles containing siRNA were capable of knocking down the target gene expression efficiently (Figure 2E).

The physicochemical properties of the nanoparticles formulated using the proposed method are shown (Figure S1). For example, when 5% PLGA and 1% PVA were used in the formulation, the average diameter was 475.9 nm. The zeta potential was measured as −23.87 mV. The diameter and zeta potential were measured using a Zetasizer (NanoZS; Malvern Panalytical, Worcestershire, UK). Field emission scanning electron microscopy (JSM-7800F, JEOL, Tokyo, Japan) was used to check whether the spheres were well formed. It was confirmed that most of the particles formed spherical wells, and a deviation in the diameter of each particle was also confirmed. The level of deviation differed by approximately 7.3 times between the minimum and

maximum and was confirmed to be an appropriate level for a bench-level study.

Among the factors that can have an effect mentioned above, the concentrations of PLGA and PVA affect the particle diameter in addition to the encapsulation rate (Figure S2). Increasing the concentration of PLGA slightly increased the encapsulation rate; however, the diameter of the formulated nanoparticles increased. If the PVA concentration was approximately 1% in PLGA with a concentration of 7.5% or higher, a particle group with a large standard deviation was formed if sonication was not sufficiently performed. In the case of sonication, the average size of the particles decreases over time; however, under certain conditions, multiple peaks may occur, in which the particles to be formulated are separated into two or more groups. When the concentration of PVA increased, the encapsulation rate increased slightly, and the average diameter of the particles increased. Several problems can occur when the PVA content is greater than 5%. If the concentration of PLGA is less than 5% in PVA (5% or more), multiple peaks may occur because of excessive sonication. When using PLGA at a concentration of 7.5% or more and PVA at a concentration of 5% or more, hardening occurred quickly and caused various problems. In this situation, if the sonication time is insufficient, the particles cannot form spheres and the polymer may clump together. In addition, it appears that multiple peaks occurred under excessive sonication.

However, the transition time from the formulation stage [2, 4] to the nanoization stage [3, 5] and the use of negatively charged microbeads seem to have a significant effect on the encapsulation rate. To confirm the effects of these two factors on the nucleic acid encapsulation rate, the formulation was prepared under the following 16 conditions. First, in the two steps [2, 4] in which negatively charged microbeads are used, 4 conditions occur, depending on whether negatively charged microbeads are used. In addition, 4 conditions occurred by dividing the conditions for the transition time to [3, 5] into 1 and 5 min. Sixteen conditions were created by multiplying the numbers of the two cases (Figure 2B). In conclusion, the shorter the conversion time to [3, 5] and the more negatively charged the microbeads, the higher the nucleic acid encapsulation rate. In addition, to visually confirm the results, the plasmid encapsulation rate of the nanoparticles formulated under the following four conditions was measured using 1% agarose gel electrophoresis. Regardless of the stage, a total of four conditions were divided into two: use of negatively charged microbeads and conversion time to nanoization in all stages: 1 and 5 min. (1) Sufficient time (5 min) before nanoization and no negatively charged microbeads. (2) Fast time to nanoization (1 min) and no negatively charged microbeads. (3) Sufficient time (5 min) before nanoization and the use of negatively charged microbeads. (4) Rapid time until nanoization (1 min) and use of negatively charged microbeads. When checking the results after electrophoresis, the highest encapsulation rate compared with the input was obtained when the conversion time to nanoization was short, and when negatively charged microbeads were used. It seems that a reduction in the transition time to step 5 has a greater effect on the improvement in the encapsulation rate than the transition time to step 3 among the transition times to nanoization. In addition, the use of negatively charged microbeads in step 4 appeared to have a greater effect on the increase in the nucleic acid encapsulation rate than the use of negatively charged microbeads in step 2.

Profile of formulated PLGA nanoparticles

For the formulated PLGA particles, it was confirmed that there was minimal size change in PBS over 24 h for both the 480 and 200 nm models (Figure S5A). This indicates that the formulated PLGA nanoparticles remain stable in PBS without significant physical change. For the 200 nm model, the encapsulation efficiency of siRNA was found to be almost similar to that of the 480 nm model (Figure 2D), indicating minimal variation in encapsulation efficiency with respect to size (Figure S5B).

In addition, the degradation of PLGA nanoparticles and the release profile of the encapsulated siRNA were assessed under specific conditions. The formulated PLGA nanoparticles were placed in PBS, 10% FBS, and mouse serum, and the extent of degradation and release profiles were measured. The degradation of PLGA nanoparticles was slowest in PBS and fastest in mouse serum. In mouse serum, it was observed that over 40% of the nanoparticles degraded within 2 days of exposure (Figure S5C). Correspondingly, siRNA release was slowest in PBS and fastest in mouse serum, with over 70% of siRNA being released after more than 50 h of exposure in mouse serum (Figure S5D).

Furthermore, the conjugation efficiency of PSMA-617 and the change in conjugation rate over time were measured. The results showed that approximately 0.73 mg out of 1 mg of input PSMA-617 was conjugated, indicating a conjugation rate of about 73% post-formulation, with the remaining 26% being quantified in the flowthrough (Figure S5E). The decoupling rate of PSMA-PLGA over time was also investigated, revealing that there was minimal decoupling of PSMA-PLGA in PBS within 24 h (Figure S5F).

Immune response and biocompatibility of PSMA-PLGA nanoparticle

The immune response to siRNA treatment delivered through PSMA-PLGA nanoparticles was assessed in a mouse model. Serum cytokine levels were analyzed 2 and 24 h after intraperitoneal injection of siRNA-containing PSMA-PLGA nanoparticles. The proinflammatory cytokines, including INF-γ, IL-1β, IL-17A, and TNF-α, showed no changes. Similarly, the levels of anti-inflammatory cytokines, including IL-10 and IL-12, were unchanged after siRNA treatment (Figure S3A). Complement activation was also assessed by measuring C5a and C3a levels in serum following siRNA treatment. The levels of C5a and C3a remained unchanged 24 h after treatment with siRNAs encapsulated into PSMA-PLGA nanoparticles (Figure S3B). Interestingly, the immune response in tumors was somewhat different. The expression of interferon-responsive genes was evaluated in tumor lysates 24 h after siRNA treatments. si*PSA* treatment doubled the mRNA expression of IFN-α, IFN-β, IFN-γ, IFNAR1, IFNGR1, and STAT1. This effect was even more pronounced in si*VEGFR2*-treated

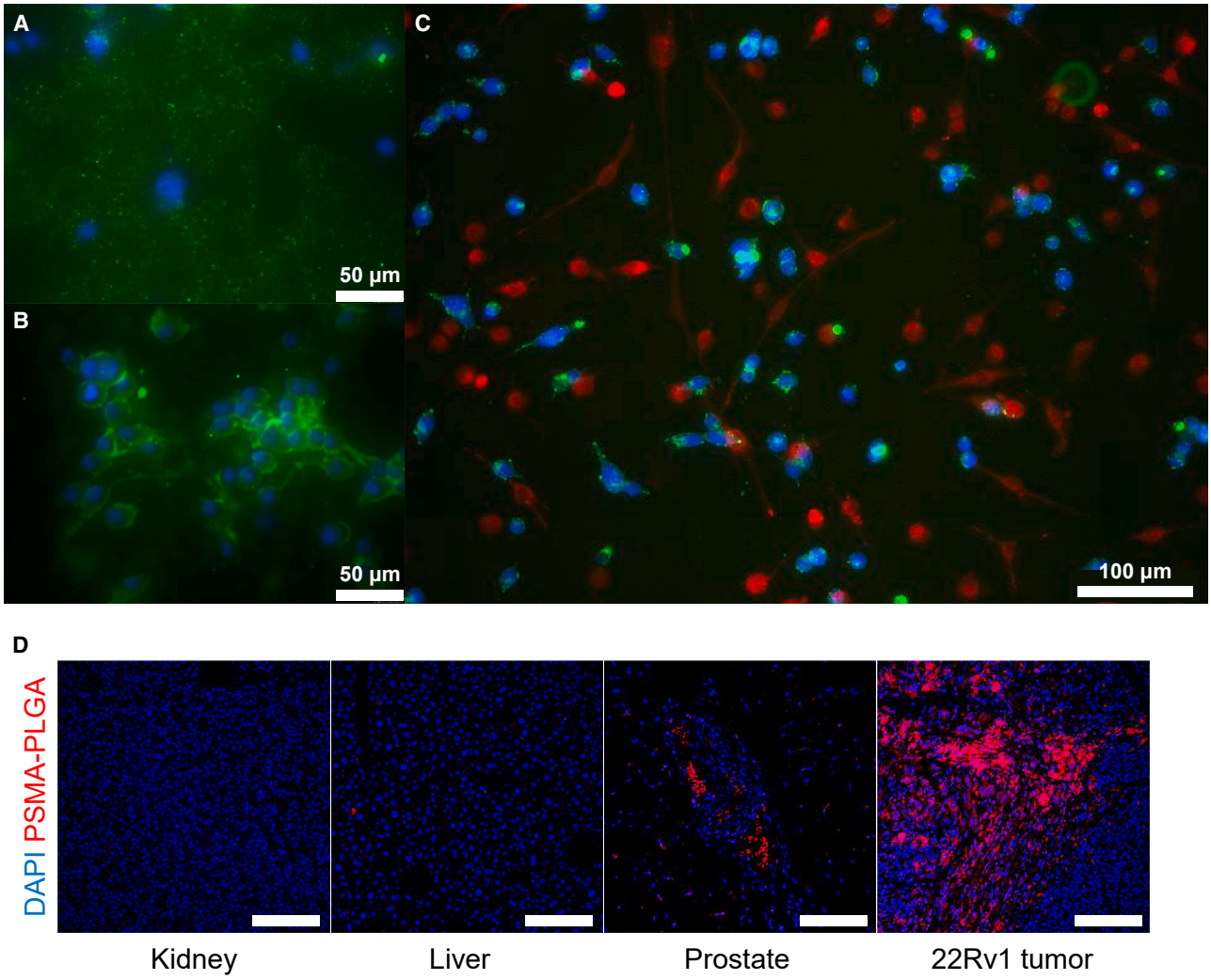

Figure 3. PSMA-PLGA precisely attach to the PSMA expressing prostate cancer cells

(A) Representative image of 22Rv1 cells treated with PLGA nanoparticles containing plasmid without PSMA conjugation. (B) Representative image of 22Rv1 cells treated with PSMA-PLGA nanoparticles containing plasmid. (C) Representative image of co-cultured 22Rv1 and C2C12 cells treated with PSMA-PLGA nanoparticles containing plasmid. Green, FITC-labeled plasmid; blue, 22Rv1; red, C2C12. (D) Representative image of each organs and tumor treated with RFP expressing PSMA-PLGA nanoparticles. Scale bars, 150 μm.

tumors, which showed significantly higher mRNA expression levels of these genes (Figure S3C). The activation of interferon-responsive genes may contribute to building anti-tumor immunity and enhancing anti-tumor effects. This finding suggests that the immune response to siRNAs was evoked in tumors specifically, and not systemically, due to the selective delivery system using PSMA-PLGA nanoparticles.

The liver enzymes and renal function were not affected by the siRNA treatments delivered through PSMA-PLGA nanoparticles (Figure S4A). In addition, there was no observed hemolytic activity associated with PSMA-PLGA nanoparticles containing siRNAs (Figures S4B and S4C).

Specificity of PSMA-PLGA nanoparticle on prostate cancer cells

To assess the targeted cellular interaction of formulated nanoparticles, a fluorescence microscope was utilized to observe the interaction between the prostate cancer cell line 22Rv1 and the nanoparticles. Specifically, PSMA-617-conjugated PLGA nanoparticles were developed to encapsulate plasmids, with the inclusion of an FITC linker to visualize the plasmid-containing nanoparticles. It was evident that nanoparticles lacking PSMA-617 conjugation did not bind to 22Rv1 cells and remained suspended (Figure 3A). In contrast, nanoparticles in the PSMA-617-conjugated state exhibited strong adherence to the 22Rv1 cells (Figure 3B). Further confirmation of the PSMA-PLGA's specific targeting capability was pursued through co-culturing experiments. Co-cultures involving myofibroblast cells

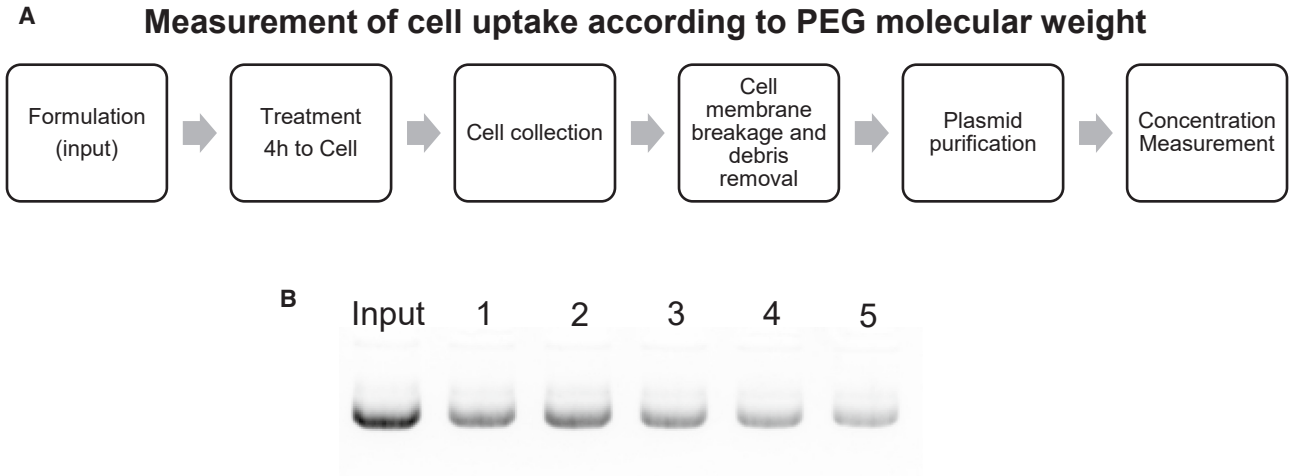

Figure 4. Intracellular uptake of PLGA nanoparticles according to the molecular weight of PEG used in the formulation

(A) Experimental procedure for measuring intracellular uptake rate. (B) The result of visually confirming how much nucleic acid entered the cells compared with the input by electrophoresis on a 1% agarose gel. The PEG molecular weight for each lane is as follows. (1) MW 2,000, (2) MW 3,000, (3) MW 6,000, (4) MW 10,000, (5) MW 20,000. PLGA, poly(lactic-co-glycolic acid); PEG, polyethylene glycol.

(C2C12 cell line) and 22Rv1 cells, a representative CRPC cell line expressing PSMA, were established. Upon treatment with plasmid-encapsulated PSMA-PLGA within this co-culture system, it was demonstrated that PSMA-PLGA selectively adhered solely to 22Rv1 cells and not to myofibroblasts (Figure 3C).

To evaluate the tissue specificity of PSMA-PLGA nanoparticles in an *in vivo* model, RFP-expressing PSMA-PLGA nanoparticles were injected intraperitoneally into a 22Rv1 tumor-bearing mouse. RFP expression was assessed in the kidney, liver, prostate, and tumors, revealing specific positive expression in prostate tissue, particularly in the 22Rv1 tumor (Figure 3D). This indicates that PSMA-PLGA nanoparticles can be specifically delivered to PSMA-positive tissues in an *in vivo* model.

Cell uptake rate according to molecular weight of PEG conjugated to nanoparticles

Polyethylene glycol (PEG) is used in polymer formulations to prevent hepatic clearance.[18] In this study, PEG was used to conjugate molecules capable of targeting membrane-specific proteins. Because the length of the PEG molecule is determined by the molecular weight of PEG, it was assumed that the cellular uptake rate of the nanoparticles could differ depending on the molecular weight of PEG. The formulated nanoparticles were used to measure the intracellular uptake rate. After treating the cultured cells with the formulated nanoparticles for 4 h, they were detached using trypsin (Gibco, Thermo Fisher, Waltham, MA). RIPA Buffer (ab156034, Abcam, Cambridge, UK) was used to destroy the cell membrane and centrifugation was performed. Only the supernatant was used to purify the plasmids. The purified plasmid was regarded as the output and the intracellular uptake rate was calculated (Figure 4A). The cells were treated with nanoparticles formulated using PEG of different molecular weights. The obtained plasmids were loaded onto each lane of a 1% agarose gel and electrophoresed. The molecular weights of the largest and smallest PEGs used were more than 10 times different between the largest and the smallest (minimum, 2 kDa; maximum, 20 kDa PEG) (Figure 4B). In conclusion, nanoparticles formulated using 3 kDa PEG showed the best cellular uptake rate, and the cellular uptake rate decreased as the molecular weight of PEG increased beyond 3 kDa.

PSMA-PLGA nanoparticles can precisely deliver siRNA to prostate tumors

The cellular proliferation of 22Rv1 cells was evaluated under treatment with siRNAs, including scrambled siRNA as a control, as well as si*PSA* and si*VEGFR2*. The si*PSA* and si*VEGFR2* were encapsulated into PSMA-PLGA nanoparticles and administered to the cells. The proliferation of 22Rv1 cells was significantly inhibited by the si*PSA* and si*VEGFR2* treatments delivered via PSMA-PLGA nanoparticles (Figure 5A).

A xenograft model was established using the 22Rv1 cell line to experiment with the delivery of siRNA *in vivo*. Each mouse was dosed with 2 μg/g of siRNAs, which were encapsulated into PLGA nanoparticles either with or without PSMA-617 conjugation. A total of six doses was administered over 2 weeks. Administration was carried out via intraperitoneal injection. Control tumors denote the use of scrambled siRNA. After the 2 weeks of treatment, tumors were harvested and analyzed for the expression of target genes according to each siRNA treatment. The immunoblot analysis revealed that intraperitoneal injection of siRNA encapsulated into PSMA-PLGA efficiently downregulated the PSA and VEGFR2 level according to si*PSA* and si*VEGFR2* RNA treatment, respectively (Figure 5B). Furthermore, si*PSA* and si*VEGFR2* specifically

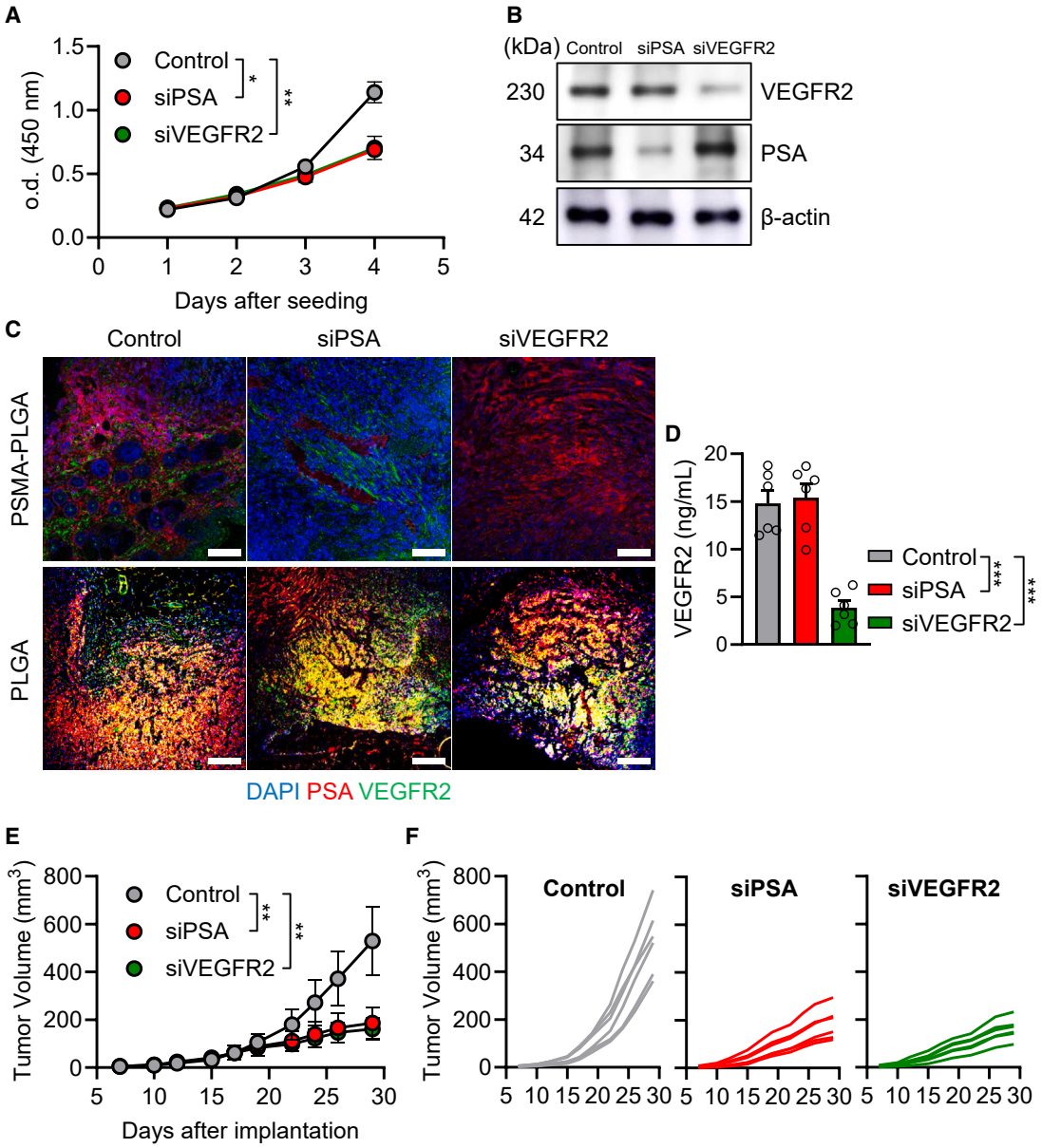

Figure 5. siRNA delivery in 22Rv1 xenograft tumor model using PSMA-PLGA nanoparticles

(A) Comparison of 22Rv1 cell proliferation following siRNA treatment. (B) Immunoblot analysis of VEGFR2, PSA, and β-actin in 22Rv1 xenograft tumors treated with indicated siRNA. (C) Representative images indicating PSA and VEGFR2 expression on 22Rv1 xenograft tumors treated with siRNAs. Scale bars, 250 μm. (D) Comparison of VEGFR2 level from 22Rv1 tumor lysates. (E) Comparison of 22Rv1 tumor growth. n = 6 mice/group from 2 independent experiment. Plot and bars indicate mean ± SD. (F) Plot indicates each individual tumor growth. $^{*}p < 0.05$, $^{**}p < 0.01$, $^{***}p < 0.001$.

diminished PSA and VEGFR2 expression, respectively, when delivered through PSMA-PLGA nanoparticles. In contrast, si*PSA* and si*VEGFR2* treatments with PLGA nanoparticles without PSMA-617 conjugation failed to reduce the target gene expression. As expected, the control tumors showed expression of PSA and VEGFR2. (Figure 5C). To ensure the effect of si*VEGFR2* in tumor tissues, the tumor lysates were analyzed with ELISA, which showed dramatically reduced expression of VEGFR2 compared with control and si*PSA*-treated tumors (Figure 5D). Interestingly the systematic treatment of siRNA using PSMA-PLGA prevented tumor growth significantly by 64.7% and 69.6%, respectively (si*PSA* and si*VEGFR2*, $p < 0.01$) (Figures 5E and 5F).

DISCUSSION

Therapeutic agents that use nucleic acids are continuously being developed for various diseases, because they can accurately remove

target genes owing to the complementarity of DNA.[19] Nucleic acid therapeutics are highly accurate but easily destroyed by enzymes and immune mechanisms.[20] Therefore, a drug delivery system capable of delivering and modifying nucleic acids to a target site is required. PLGA is a polymer that can form nano- and micro-sized spheres with desired diameters and conjugate desired molecules to the surface of nanoparticles. It is widely used in drug delivery systems. However, because the surface of the polymer is negatively charged during formulation, it is difficult to encapsulate nucleic acids with a strong negative charge in the backbone. In this study, a method for formulating PLGA nanoparticles with a high nucleic acid encapsulation rate and targeting specific cell membrane proteins was proposed. In particular, a nanoparticle formulation capable of directly targeting prostate cancer cells by targeting PSMA was designed. Factors affecting the nucleic acid encapsulation rate include the concentrations of PLGA and PVA, use of negatively charged microbeads in the formulation, and transition time from the formulation stage to the nanoization stage. The encapsulation rate slightly increased as the concentration of PLGA and PVA increased, but it seemed to have a greater effect on particle size than on encapsulation. This is thought to occur because the diameter of the formulated particles increases as the concentration of PLGA and PVA increases, and the electrical repulsive force between the polymer and nucleic acid decreases toward the center of the particle. The use of negatively charged microbeads during formulation and the transition time from the formulation stage to the nanoization stage significantly affected the nucleic acid encapsulation rate. When negatively charged microbeads are used, the encapsulation efficiency of nucleic acids is thought to increase because the polymer is expected to be positioned between the nucleic acid and negatively charged microbeads, which are expected to repel each other. Although the reason for the increase in the encapsulation rate during the transition from the formulation to the nanoization stage is unclear, it is interpreted that the physical dispersion force is greater than the electrical repulsion during the physical dispersion process. When hardening occurs due to PVA in a physically dispersed state, it is interpreted to affect the improvement in the encapsulation rate to some extent.

Although the nanoparticle formulation method presented in this study offers promising advances in targeted therapy, it has certain limitations and future perspectives that should be considered. Currently, the formulation method is at the laboratory level and requires further development to enable mass production for industrial applications. In addition, the target material attachment method demonstrated high efficiency, specifically with PSMA-617. However, additional research is necessary to explore its applicability to other materials. If the method presented in this study is further developed for industrial use, it holds great potential for widespread application in pharmaceuticals, functional food materials, and cosmetic formulations. It is crucial to address these limitations and conduct further investigations to enhance the scalability and versatility of the nanoparticle formulations for targeted therapies.

MATERIALS AND METHODS

Formulation method to encapsulate plasmid with high efficiency using PLGA

PLGA nanoparticles decompose into glycolic acid and lactic acid *in vivo* and release active substances inside the cells. The main component of nanoparticles is PLGA, which is widely used in the research and development of drug delivery systems.[2] However, the use of PLGA for nucleic acid encapsulation has several disadvantages. As PLGA is negatively charged, it is repelled by other materials with negative charge. Because nucleic acids have a strong negative charge due to the phosphate group of the backbone, it is difficult to encapsulate them using PLGA. In this study, a method for the high-efficiency encapsulation of nucleic acids in PLGA is presented.

For nucleic acid encapsulation, the overall formulation of the nanoparticles was a W/O/W formulation designed to encapsulate the plasmid inside the innermost layer. Formulation consists of a total of nine steps (Figure 1). The first step was the preparation of the encapsulated substance. In step 1, the nucleic acids (ex. DNA, RNA, plasmids, etc.) encapsulated in biodegradable nanoparticles were dissolved in an appropriate water-soluble solvent. In this study, plasmid dissolved in distilled water (DW) at a concentration of 1 μg/μL was used. The second step is the "W/O formulation" step, in which DW in which nucleic acids are dissolved (the result of 1) is dropped drop by drop into the organic solvent (a state in which PLGA, PCL, PLA, etc., are dissolved in organic solvents such as DCM (dichloromethane) and chloroform at a concentration of 2.5%–7.5%) being homogenized at high speed (more than 3,000 rpm). PLGA (P2191-5G, Sigma-Aldrich, Burlington, MA) and DCM (Sigma-Aldrich) were used in this study. It is recommended that the decrease in 1 should not exceed 5% of the total organic solvent capacity. In this process, the addition of negatively charged microbeads improves the encapsulation rate of nucleic acids. In this study, a cation-exchange resin (POROS, Thermo Fisher Scientific, Waltham, MA) was used as the negatively charged microbead. The third stage is the "Nanoization I" stage, where the result of 2 is sonicated to break the particle size down to the nano level. If it takes less than 1 min from process 2 to the start of process 3, it is helpful for improving the encapsulation rate of nucleic acids. The fourth step is the "W/O/W formulation" step, in which the product of 3 is dropped drop by drop into the PVA (Sigma-Aldrich) solution being homogenized at high speed (more than 3,000 rpm). It is recommended that the dropping result 3 should not exceed 5% of the total volume of the PVA solution (the concentration of the PVA solution used was 1%–5% PVA). In this process, the addition of negatively charged microbeads improves the encapsulation rate of nucleic acids. The negatively charged microbeads added in step 4 have a more significant effect on the encapsulation rate than those added in step 2. The fifth stage is the "Nanoization II" stage, where the result of 4 is sonicated to break the particle size down to the nano level. If it takes less than 1 min from process 4 to the start of process 5, it is helpful for improving the encapsulation rate of nucleic acids. The time until the start of sonication at that stage has a more significant effect on

the result than the same process at stage 3. The sixth step was evaporation, in which the internal organic solvent from the result of 5 was evaporated using a homogenizer (Coretech, HMZ-30DN, Anyang-si, Republic of Korea). The seventh step is the purification step, which removes the negatively charged microbeads. This process can be omitted when the negatively charged microbeads do not significantly affect the subsequent experiments. One method of removing negatively charged microbeads is the use of positively charged columns. This method can be used when a substance capable of targeting a specific cell membrane protein cannot be conjugated to the nanoparticle surface. If a positively charged column is used, a flowthrough with negatively charged microbeads removed can be obtained. The second method of removing negatively charged microbeads involves attaching excess recombinant cell membrane proteins to membranes, such as PVDF (Millipore, Burlington, MA), and attaching formulated nanoparticles to the proteins. The flowthrough was then removed, and the nanoparticles attached to the membrane were removed. This method can be used when a substance capable of targeting a specific cell membrane protein is conjugated to the nanoparticle surface. The second method has a very good degree of purification compared with the first method, but takes a long time and loses a certain volume of nanoparticles produced. Therefore, the yield can be increased by repeating the flowthrough the membrane several times. The eighth step is the "Purification II" step, where nanoparticles are precipitated by centrifugation and then washed with water three or more times. The final step is "Lyophilization," which removes most of the supernatant by centrifuging the washed nanoparticles. Then, after freezing at a temperature below −70°C, lyophilization is performed using a lyophilizer (FreeZone 6+, Labconco, Kansas City, MO).

In addition, specific cells can be targeted by conjugating an appropriate substance (antibody or a small molecule) to the nanoparticle surface. In this study, PSMA-617 (HY-117410, MedChemExpress, Monmouth Junction, NJ), which can target PSMA, a cell membrane protein in prostate cancer, was conjugated to the nanoparticle surface.[21] Specific molecules are conjugated using PEG, which is known to help avoid hepatic clearance. The conjugation of PSMA-617 to PEG can target PSMA on the surface of prostate cancer cells, thereby increasing their permeability into the tumor cells. For conjugation, PEG-NH2 (Sigma-Aldrich), which has an amine group at the PEG end, was used as the nanoparticle formulation. When the amine group of PEG-NH2 and the carboxyl group of PSMA-617 were used to form a peptide bond and conjugate, PSMA-617-conjugated PEG was produced and used for nanoparticle formulation. When a peptide bond was formed and conjugated using the amine group of PEG-NH2 and the carboxyl group of PSMA-617, PSMA-617-conjugated PEG was produced and used for nanoparticle formulation. Conjugation proceeds at the "PSMA-617 (or other targets) conjugation" step [3-2] of the entire formulation step. In the first step of conjugation, the carboxyl group of PSMA-617 was reacted with 1-ethyl-3-[3-dimethylaminopropyl]carbodiimide hydrochloride. The product was reacted with N-hydroxysuccinimide. The O-acylisourea intermediate was produced as a byproduct of the reaction, and the reaction was stopped using 2-mercaptoethanol at an appropriate level. When PEG-NH2 was added to generate a peptide bond, conjugation with the previously added reacted PSMA-617 occurred. Subsequently, the result of [3-2] is mixed with that of 3 and the subsequent 4 W/O/W formulation step proceeds.

Method for measuring plasmid and siRNA encapsulation rate by PLGA formulation

The amount of plasmid prepared in the formulation [1] step was used as the input (Figures 2A–2C). After completion of the entire formulation process, the lyophilized nanoparticles were dissolved in DCM. The amount of plasmid was considered as the output. The input and output amounts were measured using NanoDrop (ND-2000, Thermo Fisher Scientific) or agarose gel electrophoresis to calculate the encapsulation rate.

The quantification of siRNA was performed using the stem-loop RT-PCR method as described by Chen et al.[17] (Figure 2D). The quantification was carried out following the manufacturer's protocol, utilizing the TaqMan MicroRNA Reverse Transcription Kit (4366596, Applied Biosystems, Waltham, MA). The siRNA sequences and primers were designed using the AccuTarget Predesigned siRNA program (Bioneer, Daejeon, Republic of Korea).

Method for confirming target cell attachment of formulated nanoparticles

By attaching the FITC-linker to the nucleic acid, it is possible to confirm the encapsulation of the nucleic acid and its attachment to the target cell simultaneously using a fluorescence microscope (Figures 3A–3C). Nucleic Acid Labeling Reagents (MIR3225, Mirus Bio LLC, Madison, WI) were used for the FITC linker, and the attachment method was based on the corresponding reagent protocol. A Leica fluorescence microscope (DMI4000B, Leica, Wetzlar, Germany) was used. The encapsulation of nucleic acids can be confirmed by the fact that the nanoparticles emit green fluorescence. Target cell attachment was confirmed by attaching the green nanoparticles to the target cell membrane. To confirm specific attachment to the target cells, target and non-target cells were co-cultured. In this study, PSMA-617, which targets PSMA, a membrane protein in prostate cancer, was conjugated to nanoparticles. The 22Rv1 CRPC cell line was used as the target cell,[22–24] and the C2C12 cell line, a myoblast that does not express PSMA, was used as the non-target cell line. To distinguish target cells from non-target cells, target cells were stained blue, and non-target cells were stained red and co-cultured. Both cell lines were obtained from the ATCC (Manassas, VA). Before co-cultivation, C2C12 myoblasts were stained with CellTracker Red CMTPX (Thermo Fisher Scientific), and 22Rv1 cells were stained with CellTracker Blue CMHC (Thermo Fisher Scientific).

Method for measuring cell intake of PLGA nanoparticles

The lyophilized state after formulation was used as the input (Figure 4). After treating the cells with nanoparticles for more than 4 h, the cells were collected by centrifugation. Thereafter, the membrane was destroyed and centrifuged again to remove sinking debris, and the supernatant was separated and purified. A plasmid preparation

kit (Invitrogen, Waltham, MA) was used for preparation. The amount of purified plasmid was used as the output. Electrophoresis was performed on a 1% agarose gel to determine the amount of plasmids entering the cells compared with the input.

Cell lines and culture

In this study, the prostate cancer cell lines 22Rv1 and LNCaP, as well as the myoblast C2C12, were employed. All three cell lines were purchased from ATCC. They were cultured at 37°C in a 5% environment using RPMI-1640 medium. The medium composition included 10% FBS (Gibco, Thermo Fisher) and 1% antibiotic-antimycotic (Gibco, Thermo Fisher). To verify the selective binding of formulated nanoparticles, co-cultures of 22Rv1 and C2C12 cell lines were conducted. For the intracellular delivery of siRNA experiments, the 22Rv1 and LNCaP cell lines were utilized. The 22Rv1 cell line was also used in cytotoxicity assays and in the construction of xenograft models.

Method for confirming siRNA delivery in cell lines and animal models

To verify siRNA delivery in cell lines, prostate cancer cell lines 22Rv1 and LNCaP were employed. Both types of prostate cancer cell lines were acquired from ATCC. The 22Rv1 and LNCaP cell lines were cultured for 48 h after treatment with PSMA-617-conjugated PLGA nanoparticles, using RPMI-1640 medium. During the cultivation period, the LNCaP cell line was treated with 10 nM DHT. The target mRNAs for the treated siRNA are *PSA* and *VEGFR2*, respectively. After 48 h of nanoparticle treatment, cells were collected and total RNA was extracted using TRIzol (Thermo Fisher Scientific). Subsequently, a cDNA synthesis process was conducted. This was followed by performing qPCR to confirm the knockdown of the target mRNA. The TOPscript cDNA synthesis kit (Ezynomics, Daejeon, Republic of Korea) was used for cDNA synthesis, and the SYBR Green quantitative RT-qPCR kit (Sigma-Aldrich) was used for qPCR. The siRNA and primers for *PSA* and *VEGFR2* used in the experiments were designed and manufactured by Bioneer's AccuTarget Predesigned siRNA program (Bioneer).

The experiments on mice were conducted in accordance with the approval (24-0066-S1A0(1)) from the Institutional Animal Care and Use Committee of Seoul National University Hospital. To investigate siRNA delivery *in vivo*, a xenograft model was established using the 22Rv1 cell line. For the construction of the xenograft model, male BALB/c-nude mice, 6 weeks old, were utilized. Each mouse was injected subcutaneously with 1×10^7 cells mixed 1:1 with Matrigel (BD, Franklin Lakes, NJ). Treatment with PSMA-617-conjugated PLGA nanoparticles was initiated once the average tumor volume reached 100 mm^3, administered via intraperitoneal injection six times over a 2-week period. Tumor volume was measured thrice weekly using Vernier calipers, and tumor weight was assessed post-necropsy. Following necropsy, 50 mg of tumor tissue from each mouse was collected and grouped for analysis. Protein was then isolated from these samples for the assessment of siRNA delivery and knockdown via western blotting. In addition, the embedded tumor tissues were used for immunohistochemistry studies. The reduction of VEGFR2 by siRNA in the xenograft model was additionally quantified using the VEGFR2 Mouse ELISA Kit (EMVEGFR2, Invitrogen).

Method for conducting immunohistochemistry experiments using a confocal microscope

Tumor tissues, as well as kidney, liver, and prostate tissues obtained from a necropsy of the 22Rv1 xenograft model, were fixed, processed for tissue processing, and embedded. Paraffin blocks were sectioned to prepare slides. For immunohistochemistry, the paraffin on the slides was melted at 60°C for 20 min. Subsequently, a rehydration process was carried out. Initially, the slides were kept in xylene for 30 min, then changed to fresh xylene for 5 min, three times. Thereafter, the slides were treated for 5 min each in a solution of xylene and ethanol in a 1:1 ratio, 100% ethanol, 95% ethanol, 85% ethanol, and 75% ethanol. They were then rehydrated in DW for 2 min. Afterward, the slides were placed in 10 mM citrate (pH 6.0) containing 0.05% Tween 20 and heated at 80°C for 20 min for antigen retrieval, then cooled to room temperature. They were washed twice for 2 min each in PBST. Blocking was done at room temperature for 1 h in PBS containing 0.05% Triton X-100 and 5% goat serum. The primary antibodies were treated overnight at 4°C in PBST with 1% goat serum at a 1:50 ratio. The primary antibodies were as follows: anti-PSA (ab140337, Abcam), anti-VEGFR2 (ab115805, Abcam). After three 2-min washes in PBST, the secondary antibodies were attached. The secondary antibodies were treated at room temperature for 30 min at a ratio of 1:200 for antibodies and 1:1,000 for DAPI. The secondary antibodies were as follows: anti-rabbit IgG H&L (ab150077, Abcam), anti-mouse IgG H&L (ab150115, Abcam). Following three more 2-min washes in PBST, an anti-fading solution (ab104135, Abcam) was applied, and the slides were covered with a cover glass. The slides were then imaged using the confocal equipment Leica STED CW (Leica Microsystems).

Measurement method of PLGA nanoparticle degradation and siRNA release profile

The degradation extent of the nanoparticles was measured using the mass loss method. An initial mass of 1 mg of nanoparticles was used for each condition. The nanoparticles were incubated at 37°C in mouse serum, 10% FBS, and PBS. Subsequently, the solvent was removed, and the dried mass of the precipitated nanoparticles was measured. Measurements were taken at 24-h intervals over 10 days. The degradation extent of the nanoparticles was determined by the ratio of remaining mass to initial mass.

To measure the release of siRNA, si*PSA* was encapsulated in PLGA nanoparticles. An initial amount of 1 μg of si*PSA* was encapsulated, and the release extent was measured using stem-loop RT-PCR. The released siRNA was measured based on the supernatant remaining after the precipitated nanoparticles were removed. Measurements were taken every 12 h, up to a final time point of 144 h.

Measurement of immune response profiling induced by treatment with PSMA-PLGA nanoparticles encapsulating siRNAs

Blood was collected via cardiac puncture for the assessment of cytokine and complement changes after nanoparticle injection. For cytokine analysis, blood was drawn at 2 and 24 h post-injection to evaluate both acute and mid-term responses of pro-inflammatory and anti-inflammatory cytokines. Complement changes were measured 24 h after nanoparticle injection. The collected blood was coagulated, and serum was separated for each analysis. Cytokines were measured using the Luminex 200 Instrument System (Invitrogen) at the Protein Immunology Core Facility of the Translational Research Institute, Seoul National University Hospital. For complement analysis, C5a and C3a levels were measured using the Mouse Complement Component C5a DuoSet ELISA (DY2150, R&D Systems, Minneapolis, MN) and the Mouse Complement C3a ELISA Kit (Colorimetric) (NBP2-70037, Novus Biologicals, Centennial, CO), respectively. The relative mRNA levels of interferon-responsive genes were measured by qPCR from RNA isolated from the tumor tissues of the 22Rv1 xenograft model.

Measurement of bio-compatibility induced by treatment with PSMA-PLGA nanoparticles encapsulating siRNAs

Each siRNA was encapsulated in PSMA-617-conjugated PLGA nanoparticles. The encapsulated siRNAs were injected intraperitoneally at a dose of 2 μg/g per mouse. For hepatotoxicity evaluation, blood was collected via cardiac puncture after nanoparticle injection. Aspartate aminotransferase and alanine aminotransferase levels in the obtained serum were measured at 340 nm using colorimetric assay kits (BioSystems, Cairo, Egypt). In addition, serum creatinine levels were measured at 490 nm using a Creatinine-Colorimetric kit (MDSS, Hannover, Germany).

The measurement of hemolysis for hematocompatibility assessment was conducted as follows. Fresh whole blood was anticoagulated using ethylenediaminetetraacetic acid dipotassium salt and then diluted with 0.9% saline. Samples at different concentrations were then added and incubated at 37°C for 1 h. Saline (0.9%) was used as the negative control, and DW was used as the positive control. After incubation, the supernatant was collected by centrifugation and measured at 545 nm using an ultraviolet-visible spectrophotometer (DU800, Beckman Coulter, Brea, CA). The hemolytic activity was calculated as the percentage difference between the absorbance of the test sample and the negative control, divided by the difference between the absorbance of the positive control and the negative control.

Measurement of coupling efficiency and time-dependent decoupling of PSMA-617

To measure the conjugation efficiency of PSMA-617 during the formulation of nanoparticles, the formed nanoparticles were precipitated, re-dissolved, and the amount of PSMA in the solution was quantified. In addition, the amount of PSMA in the supernatant, excluding the precipitated particles, was quantified to measure the amount of uncoupled PSMA remaining. To determine if decoupling occurs after formulation, the nanoparticles were placed in PBS for 1, 6, 12, and 24 h, followed by precipitation and dissolution to quantify the amount of released PSMA. The quantification of PSMA was conducted using NMR at the Korea Polymer Testing and Research Institute.

DATA AND CODE AVAILABILITY

The data that support the findings of this study are available on request from the corresponding author.

ACKNOWLEDGMENTS

This work was supported by the New Faculty Startup Fund from Seoul National University. This work was funded by Korea Health Industry Development Institute (project no.: HI23C1575).

AUTHOR CONTRIBUTIONS

Conceptualization, S.H., S.-H.J., and C.K.; data curation, S.H., J.H.H., H.D.Y., C.W.J., and J.H.K.; formal analysis, S.H., S.-H.J., J.H.H., H.D.Y., C.W.J., J.H.K., and C.K.; investigation, S.H., S.-H.J., and C.K.; project administration, S.H., S.-H.J., and C.K.; methodology, S.H.; validation, S.H., S.-H.J., J.H.H., H.D.Y., C.W.J., and J.H.K.; visualization, S.H. and S.-H.J.; writing – original draft, S.H., S.-H.J., and C.K.; funding, S.-H.J. and C.K.; resources, C.K.

DECLARATION OF INTERESTS

The authors declare no competing interests.

SUPPLEMENTAL INFORMATION

Supplemental information can be found online at https://doi.org/10.1016/j.omtn.2024.102322.

REFERENCES

1. Rocha, C.V., Gonçalves, V., da Silva, M.C., Bañobre-López, M., and Gallo, J. (2022). PLGA-Based Composites for Various Biomedical Applications. Int. J. Mol. Sci. *23*, 2034.
2. Nevedomskaya, E., Baumgart, S.J., and Haendler, B. (2018). Recent Advances in Prostate Cancer Treatment and Drug Discovery. Int. J. Mol. Sci. *19*, 1359.
3. Vilella, A., Ruozi, B., Belletti, D., Pederzoli, F., Galliani, M., Semeghini, V., Forni, F., Zoli, M., Vandelli, M.A., and Tosi, G. (2015). Endocytosis of Nanomedicines: The Case of Glycopeptide Engineered PLGA Nanoparticles. Pharmaceutics *7*, 74–89.
4. Harguindey, A., Domaille, D.W., Fairbanks, B.D., Wagner, J., Bowman, C.N., and Cha, J.N. (2017). Synthesis and Assembly of Click-Nucleic-Acid-Containing PEG-PLGA Nanoparticles for DNA Delivery. Adv. Mater. *29*, 1700743.
5. Nikam, R.R., and Gore, K.R. (2018). Journey of siRNA: Clinical Developments and Targeted Delivery. Nucleic Acid Ther. *28*, 209–224.
6. Zhang, J., and Salaita, K. (2021). Smart Nucleic Acids as Future Therapeutics. Trends Biotechnol. *39*, 1289–1307.
7. Sekhoacha, M., Riet, K., Motloung, P., Gumenku, L., Adegoke, A., and Mashele, S. (2022). Prostate Cancer Review: Genetics, Diagnosis, Treatment Options, and Alternative Approaches. Molecules *27*, 5730.
8. Zhang, H., Koumna, S., Pouliot, F., Beauregard, J.M., and Kolinsky, M. (2021). PSMA Theranostics: Current Landscape and Future Outlook. Cancers *13*, 4023.
9. Seifert, R., Alberts, I.L., Afshar-Oromieh, A., and Rahbar, K. (2021). Prostate Cancer Theranostics: PSMA Targeted Therapy. Pet. Clin. *16*, 391–396.
10. Plichta, K.A., Graves, S.A., and Buatti, J.M. (2021). Prostate-Specific Membrane Antigen (PSMA) Theranostics for Treatment of Oligometastatic Prostate Cancer. Int. J. Mol. Sci. *22*, 12095.
11. Schatten, H. (2018). Brief Overview of Prostate Cancer Statistics, Grading, Diagnosis and Treatment Strategies. Adv. Exp. Med. Biol. *1095*, 1–14.

12. Wang, G., Zhao, D., Spring, D.J., and DePinho, R.A. (2018). Genetics and biology of prostate cancer. Genes Dev. *32*, 1105–1140.

13. Nguyen-Nielsen, M., and Borre, M. (2016). Diagnostic and Therapeutic Strategies for Prostate Cancer. Semin. Nucl. Med. *46*, 484–490.

14. Dördelmann, G., Kozlova, D., Karczewski, S., Lizio, R., Knauer, S., and Epple, M. (2014). Calcium phosphate increases the encapsulation efficiency of hydrophilic drugs (proteins, nucleic acids) into poly(d,l-lactide-co-glycolide acid) nanoparticles for intracellular delivery. J. Mater. Chem. B *2*, 7250–7259.

15. Shinde, V.R., Revi, N., Murugappan, S., Singh, S.P., and Rengan, A.K. (2022). Enhanced permeability and retention effect: A key facilitator for solid tumor targeting by nanoparticles. Photodiagnosis Photodyn. Ther. *39*, 102915.

16. Carol, Y., Maha, M.A., Ahmed, H.E., and Omaima, N.E.G. (2018). Ultrahigh verapamil-loaded controlled release polymeric beads using superamphiphobic substrate: D-optimal statistical design, *in vitro* and *in vivo* performance. Drug Deliv. *25*, 1448–1460.

17. Chen, C., Ridzon, D.A., Broomer, A.J., Zhou, Z., Lee, D.H., Nguyen, J.T., Barbisin, M., Xu, N.L., Mahuvakar, V.R., Andersen, M.R., et al. (2005). Real-time quantification of microRNAs by stem–loop RT–PCR. Nucleic Acids Res. *33*, e179.

18. Yin, L., Pang, Y., Shan, L., and Gu, J. (2022). The In Vivo Pharmacokinetics of Block Copolymers Containing Polyethylene Glycol Used in Nanocarrier Drug Delivery Systems. Drug Metab. Dispos. *50*, 827–836.

19. Corey, D.R., Damha, M.J., and Manoharan, M. (2022). Challenges and Opportunities for Nucleic Acid Therapeutics. Nucleic Acid Ther. *32*, 8–13.

20. Herkt, M., and Thum, T. (2021). Pharmacokinetics and Proceedings in Clinical Application of Nucleic Acid Therapeutics. Mol. Ther. *29*, 521–539.

21. Rini, B.I., and Small, E.J. (2002). Hormone-refractory Prostate Cancer. Curr. Treat. Options Oncol. *3*, 437–446.

22. Gheorghe, G.S., Hodorogea, A.S., Ciobanu, A., Nanea, I.T., and Gheorghe, A.C.D. (2021). Androgen Deprivation Therapy, Hypogonadism and Cardiovascular Toxicity in Men with Advanced Prostate Cancer. Curr. Oncol. *28*, 3331–3346.

23. Chandrasekar, T., Yang, J.C., Gao, A.C., and Evans, C.P. (2015). Mechanisms of resistance in castration-resistant prostate cancer (CRPC). Transl. Androl. Urol. *4*, 365–380.

24. Henríquez, I., Roach, M., 3rd, Morgan, T.M., Bossi, A., Gómez, J.A., Abuchaibe, O., and Couñago, F. (2021). Current and Emerging Therapies for Metastatic Castration-Resistant Prostate Cancer (mCRPC). Biomedicines *9*, 1247.